rapid communication

A comprehensive equation for the pulmonary pressure-volume curve

JOSÉ G. VENEGAS, R. SCOTT HARRIS, AND BRETT A. SIMON
Departments of Anesthesia and Critical Care, and Pulmonary Unit, Department of Medicine, Massachusetts General Hospital, Harvard Medical School, Boston, Massachusetts 02114

Venegas, José G., R. Scott Harris, and Brett A. Simon. A comprehensive equation for the pulmonary pressure-volume curve. *J. Appl. Physiol.* 84(1): 389–395, 1998.—Quantification of pulmonary pressure-volume (P-V) curves is often limited to calculation of specific compliance at a given pressure or the recoil pressure (P) at a given volume (V). These parameters can be substantially different depending on the arbitrary pressure or volume used in the comparison and may lead to erroneous conclusions. We evaluated a sigmoidal equation of the form, $V = a + b[1 + e^{-(P-c)/d}]^{-1}$, for its ability to characterize lung and respiratory system P-V curves obtained under a variety of conditions including normal and hypocapnic pneumoconstricted dog lungs ($n = 9$), oleic acid-induced acute respiratory distress syndrome ($n = 2$), and mechanically ventilated patients with acute respiratory distress syndrome ($n = 10$). In this equation, a corresponds to the V of a lower asymptote, b to the V difference between upper and lower asymptotes, c to the P at the true inflection point of the curve, and d to a width parameter proportional to the P range within which most of the V change occurs. The equation fitted equally well inflation and deflation limbs of P-V curves with a mean goodness-of-fit coefficient (R^2) of 0.997 ± 0.02 (SD). When the data from all analyzed P-V curves were normalized by the best-fit parameters and plotted as $(V - a)/b$ vs. $(P - c)/d$, they collapsed into a single and tight relationship ($R^2 = 0.997$). These results demonstrate that this sigmoidal equation can fit with excellent precision inflation and deflation P-V curves of normal lungs and of lungs with alveolar derecruitment and/or a region of gas trapping while yielding robust and physiologically useful parameters.

mechanical properties; lung compliance; lung recoil; acute respiratory distress syndrome; pneumoconstriction

QUASI-STATIC PRESSURE-VOLUME (P-V) curves have been used in research and in the clinical setting to quantify the elastic properties of the lungs and respiratory system, particularly with respect to changes in surfactant composition (1, 17, 23), lung recoil (7, 19, 25), and degree of alveolar derecruitment (24). Quantification of the curve typically consists of the compliance or specific compliance from the slope of the curve at a given pressure or over some volume range, the measurement of recoil pressure at a given fractional volume, or the measurement of the fractional lung volume remaining at a given inflation pressure. However, because of the nonlinear shape of the P-V curve, the values of these parameters and the changes observed in these parameters can vary substantially depending on the arbitrary pressure or volume used in the comparison. Furthermore, accurate estimation of these parameters may require the collection of data at precise points of the curve or, if such data are not available, extrapolation of the data within a section of the P-V curve, while a substantial fraction of the data is ignored.

Describing the lower portion of the P-V curve could also be important in the management of patients with the acute respiratory distress syndrome (ARDS). The inflation limb of the respiratory system P-V curve has recently been proposed to identify a safe range of ventilatory pressures during mechanical ventilation in patients with ARDS (2, 26). It has been postulated that ventilator-induced lung injury, occurring in ARDS, is caused by overdistension of alveoli at high transpulmonary pressures and/or by increased forces caused by the repetitive recruitment and derecruitment of alveolar units (10, 18, 31, 32). In ARDS the inflation limb of the P-V curve has a sigmoidal shape, with a point of rapid change in upward curvature, which will be referred to as "lower corner pressure" (P_{cl}),[1] and a point of rapid change in downward curvature, which will be referred to as "upper corner pressure" (P_{cu}). Physiologically, P_{cl} is thought to correspond to the pressure at which a maximal alveolar recruitment occurs, whereas P_{cu} is thought to represent the pressure above which maximal elastic distension of the lung parenchyma is approached. Mechanical ventilation delivered with airway pressures kept within the range from P_{cl} to P_{cu} is thought to limit alveolar overdistension and maximize recruitment of alveolar units (2, 26). In practice, these points of maximum curvature are often determined by eye from a plot of the P-V curve, a method that is not only imprecise, but also highly subjective.

Curve fitting of the P-V relationship is one approach to solving these problems. The curve fit permits more accurate extrapolation of the curve over a desired data range. To facilitate comparisons between curves obtained from different subjects or under changing conditions, the volume data are often normalized by total lung capacity (TLC), defined as the lung volume at an

[1] This pressure is often referred to as "lower inflection point" in the literature (2, 20, 26). Strictly speaking, the inflection point of a curve is the point at which the curvature changes direction or sign and not the point of maximum curvature.

arbitrary inflation pressure ranging from 25 to 40 cmH_2O (4). Because individual data sets rarely reach the exact maximum pressure, TLC values may be more objectively obtained by curve fitting the data. In addition, physiologically meaningful parameters obtained from the fitted model may better characterize the P-V curve over its full range, rather than at an arbitrary specified point. Although only valid for volumes >50% TLC (27), the exponential equation proposed by Salazar and Knowles (28) has been most widely utilized to characterize these volumes, and the parameters thus obtained correlated with changes in pulmonary elasticity with aging and smoking (5, 6, 9) and with emphysema, asthma, and interstitial fibrosis (13–15). The lower portion of the curve, which has relevance for assessing alveolar recruitment and air trapping, is not described by these models. Polynomial and other models that describe the entire P-V curve have been limited by the lack of physiological significance of the parameters (8).

Fitting an equation to experimental or clinical P-V data provides a systematic method to characterize P-V curves and derive objective parameters from them. The purpose of this communication is to present a simple form of a sigmoidal equation that fits with remarkable accuracy the inflation and deflation limbs of P-V curves obtained under a variety of experimental and pathological conditions and yields physiologically useful parameters. When the pressure and volume data are expressed in dimensionless form normalized by parameters obtained from the model, the data collapse onto a single comprehensive P-V relationship.

METHODS

A sigmoidal equation of the static P-V curve was formulated as

$$V = a + \left[\frac{b}{1 + e^{-(P-c)/d}}\right] \quad (1)$$

where V is inflation or absolute lung volume, P is airway opening or transpulmonary pressure, and *a*, *b*, *c*, and *d* are fitting parameters. Each of these parameters has a physiological correlate (Fig. 1). The parameter *a* has units of volume and corresponds to the lower asymptote volume, which approximates residual volume when absolute lung volume and airway opening pressure are used as units. The parameter *b*, also in units of volume, corresponds to the vital capacity or the total change in volume between the lower and the upper asymptotes. The parameter *c* is the pressure at the inflection point of the sigmoidal curve (where curvature changes sign) and also corresponds to the pressure at the point of highest compliance. Finally, the parameter *d* is proportional to the pressure range within which most of the volume change takes place. The pressures at which the function rapidly changes slope, which we will call lower and upper corner points (P_{cl} and P_{cu}), can be defined from the intersections between a tangent to the P-V curve at the point of maximal compliance ($P = c$) and the lower and upper asymptotes, respectively. In *Eq. 1* these points can be directly obtained as a function of *c* and *d* as

$$P_{cl} = c - 2d$$

$$P_{cu} = c + 2d$$

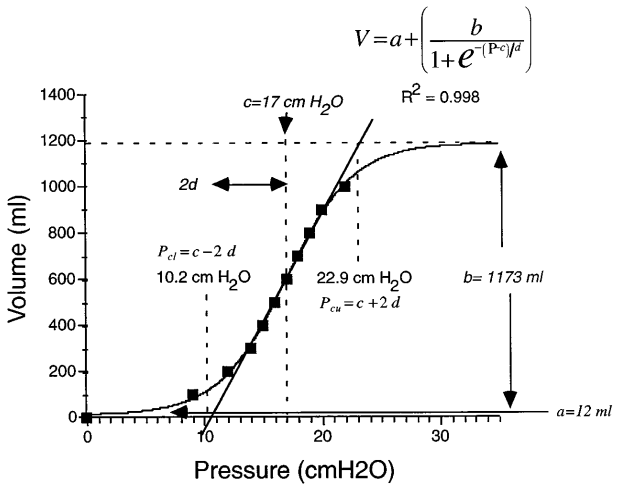

Fig. 1. Inflation pressure-volume (P-V) data measured in a patient with acute respiratory distress syndrome (ARDS) and fitted to *Eq. 1*. Corner points, P_{cl} and P_{cu}, can be calculated from parameters *c* and *d* obtained from fitting. Fitting parameters are represented by *a*, *b*, *c*, and *d*.

We assessed the adequacy of this equation by fitting it to P-V data previously obtained from intubated and mechanically ventilated lungs under various pathophysiological conditions (Table 1). We analyzed inflation and deflation lung P-V curves obtained from a supine dog before and 30 and 60 min after inducing acute lung injury by intravenous injection of oleic acid (0.1 ml/kg). We also analyzed inflation limb P-V data of the respiratory system of 10 mechanically ventilated ARDS patients and deflation P-V data for the right and left lungs from 11 open-chest dogs after unilateral pneumoconstriction created by total occlusion of the left pulmonary artery (PA) (30).

Inflation limbs of the P-V curves were obtained by manual inflation with calibrated syringes in 8–10 discrete volume steps until an airway opening pressure (Pao) close to 30 cmH_2O was reached. Deflation limbs of the P-V curves were obtained after an inflation to TLC by withdrawing volume in discrete steps back to atmospheric airway pressure. For each lung volume, Pao was recorded after ~5 s to allow the pressure to reach a quasi-steady-state value. Data from dogs in which ARDS was induced by intravenous infusion of oleic acid consisted of transpulmonary pressure, calculated as Pao minus esophageal pressure, vs. total absolute lung volume, estimated as inflation volume plus functional residual capac-

Table 1. *Data analyzed*

	n	System	PV Limb	Condition
Intact-chest dogs	2	Lung	Inflation and deflation	Control and ARDS (30 and 60 min post-oleic acid injury)
Patients	10	Respiratory	Inflation	Mechanical ventilation ARDS
Open-chest dogs	11	Right lung	Deflation	Open chest
		Left lung	Deflation	Pneumoconstriction by left PA occlusion

Data collection complied with policies of the Institutional Review Board and Institutional Animal Care and Use Committee of Massachusetts General Hospital. ARDS, acute respiratory distress syndrome; PA, pulmonary artery.

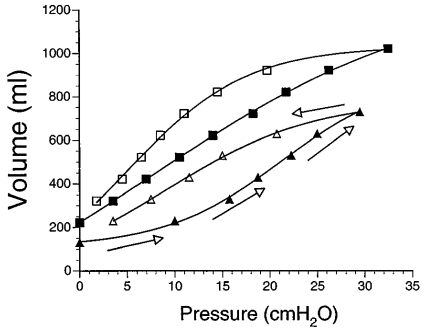

Fig. 2. Inflation (filled symbols) and deflation (open symbols) P-V data for a dog before (squares) and 60 min after (triangles) oleic acid-induced lung injury. Solid lines, curves obtained by fitting *Eq. 1* to each data set. $R^2 > 0.997$ in all cases.

ity (FRC) measured by helium dilution. Human data consisted of inflation volume above FRC plotted against Pao. Left lung PA-occluded open-chest dog data consisted of absolute lung volume, measured with a positron camera, vs. Pao (30). P-V curves were fitted by *Eq. 1* in a personal computer using the Levenberg-Marquardt iterative algorithm to minimize the sum of squared residuals. The algorithm was set to run until the resulting sum of squared residuals changed by <0.0001, yielding estimates of the parameters *a*, *b*, *c*, and *d* and the best-fit coefficient R^2.

RESULTS

Equation 1 fitted equally well inflation and deflation P-V curves from normal, ARDS, and pneumoconstricted lungs (Figs. 1–3) with mean goodness-of-fit coefficient (R^2) of 0.997 ± 0.02 (SE). Review of the fitted parameters revealed the following results. In the dog lung the inflation P_{cl} increased from a negative value (-21 cmH_2O) to positive values of 3.2 and 8.7 cmH_2O at 30 and 60 min after induction of ARDS. In 8 of the 10 ARDS patients, inflation limb P_{cl} was also greater than zero [9 ± 6 (SD) cmH_2O]. The other two patients had a negative inflation limb P_{cl} (average -23 cmH_2O). In the left PA-occluded dogs the inflection point, *c*, occurred at a significantly greater pressure ($P < 0.05$) in the occluded left lung (5 ± 0.46 cmH_2O) than in the control right lung (0.78 ± 1.55 cmH_2O). When the data from all analyzed P-V curves were normalized by the parameters derived by the fitting and plotted as $(V - a)/b$ vs. $(P - c)/d$, they collapsed into a tight relationship (Fig. 4) closely following *Eq. 1* ($R^2 = 0.997$) and with residuals evenly scattered within a 5% range (Fig. 5).

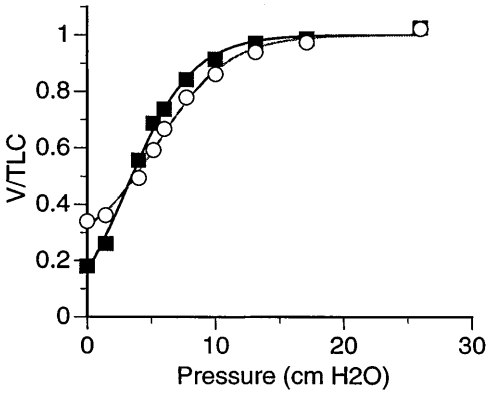

Fig. 3. Representative example of deflation P-V data for right lung (■) and left-pulmonary artery-occluded lung (○). Lines represent best fit of *Eq. 1*. TLC, total lung capacity. $R^2 = 0.997$ and 0.995, respectively. (Adapted from Fig. 5 in Ref. 30.)

DISCUSSION

The major finding of this study is that a simple sigmoidal equation (*Eq. 1*) fitted with excellent accuracy the inflation and deflation limbs of experimental and clinical P-V curves obtained under a variety of experimental and pathological conditions ($R^2 = 0.997$). Furthermore, when the pressure and volume data are expressed in dimensionless form and plotted as $(V - a)/b$ vs. $(P - c)/d$, they collapse onto a comprehensive P-V relationship.

For obvious reasons, the sensitivity of the fitting to parameters that depend on data not available is inherently poor, and fitted values of these parameters are unreliable. For example, in Fig. 2 the upper asymptote of the inflation limb in ARDS is never reached, and thus the parameter *b* obtained from the fitting is not reliable, even though the parameters *a*, *c*, and *d* may be. This limitation should not restrict the usefulness of the equation, since *1*) as discussed above in most cases it is not practical, or even desirable, to obtain complete data sets from both asymptotes and *2*) only parameters sensitive to data within the measured range are those generally sought. As with any equation, it is important to be aware of this limitation and conduct a parameter-sensitivity analysis to assess the reliability of the parameters estimated from the curve fit (11).

An important feature of *Eq. 1* is the ability to objectively characterize the P-V relationship and obtain accurate estimates of physiologically relevant parameters. For example, compliance at any pressure or volume, the first derivative of the equation, can be expressed as

$$\frac{\partial V}{\partial P} = \frac{b}{d} \frac{e^{-(P-c)/d}}{[1 + e^{-(P-c)/d}]^2} \qquad (2)$$

From *Eq. 2*, maximal compliance, or the compliance at the "most linear" portion of the P-V curve, occurs at $P = c$ and is equal to $b/4d$.

Recently, there has been increasing interest in the lower and upper portions of the P-V relationship as regions possibly representing recruitment and overdistension of alveoli, respectively. This notion has gained acceptance clinically in ARDS patients as a way to identify safe limits of ventilatory pressures for mechanical ventilation. In the literature, actual P_c values have been derived by eye from plotted P-V data, and the definitions for them have been inconsistent. P_c has been defined as the points at which the P-V curve consistently separates from a straight line drawn through the most linear portion of the curve (24) or where such a line intersects with lines drawn tangent to the P-V curve at the lowest and highest pressures measured (2, 12). We chose to define P_c as the intersections between a tangent to the P-V curve at its point of maximum compliance (inflection point, *c*) and the two horizontal

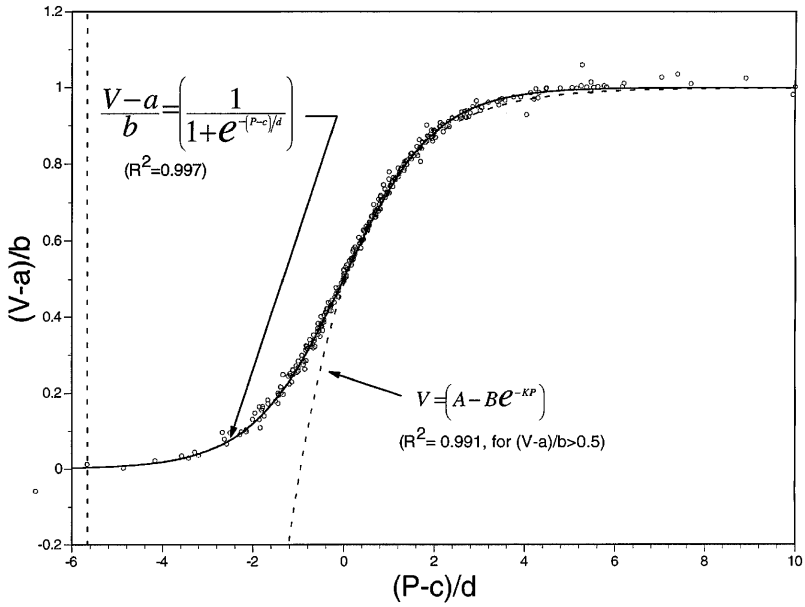

Fig. 4. Volume (V) normalized by fitted parameters a and b plotted against pressure (P) normalized by fitted parameters c and d. Data points (n = 406) include deflation data from intact right lungs and pneumoconstricted pulmonary artery-occluded left lungs (9 dogs), inflation data of 10 patients with ARDS, and inflation and deflation data from 2 dogs before and after oleic acid-induced lung injury. P-V data collapse into a single comprehensive relationship following *Eq. 5* (solid line) and clearly departing from exponential *Eq. 3* (dashed line) for volumes <50% of vital capacity.

asymptotes a and b, which can be readily derived from *Eq. 1* as $P_c = c \pm 2d$. Although this definition resembles that from Amato et al. (2), *Eq. 1* could also be used to define P_c in different ways: as the points of maximal upward and downward curvature of the P-V curve ($P_c = c \pm 1.317d$), or as the points of maximal rate of change of curvature ($P_c = c \pm 2.29d$). A clinically optimal definition of P_c remains to be determined.

The following results further illustrate the usefulness of *Eq. 1*. In the normal lung, alveolar derecruitment at FRC should be minimal, whereas in ARDS, derecruitment should be substantially increased. If the location of P_{cl} on the x-axis reflects the pressure at which rapid alveolar recruitment begins, then in the normal lung P_{cl} should be negative, whereas in ARDS P_{cl} should be shifted to the right and positive. In the dog lung P_{cl} shifted from a negative value in control conditions to a positive value 60 min after induction of ARDS. Similarly, in eight of the ARDS patients P_c was greater than zero. These results are therefore consistent with the substantial alveolar derecruitment expected at low levels of lung inflation in ARDS. In the unilaterally left PA-occluded dogs the inflection point, c, was substantially greater in the PA-occluded lung than in the control right lung. This is consistent with the increase in lung recoil, measured at 50% TLC (30), of the PA-occluded lung caused by hypocapnic pneumoconstriction. However, the difference in lung recoil between the left and right lungs, measured as the horizontal distance between the two curves, is highly dependent on the standard volume selected in the comparison (Fig. 3).

Other P-V equations. A detailed discussion of equations used to fit P-V data was presented by Murphy and Engel (20). Of these, the exponential function originally proposed by Salazar and Knowles (28) has the form

$$V = (A - Be^{-kP}) \quad (3)$$

where the parameter A, corresponding to TLC, and the parameters B and k reflect the elastic stiffness of the lung. *Equation 3* has been widely used to characterize the inflation and deflation limbs of normal human and animal lungs (29) and of lungs affected by several types of diseases, such as emphysema, asthma, fibrosis, and sarcoidosis (13–15). *Equation 3* fits the P-V data well for lung volumes >50% of TLC. This is clearly shown in our data, which were well fitted by *Eq. 3* for values of $(V - a)/b > 0.5$ (R^2 = 0.993; Fig. 4). This agreement is not surprising, since in the upper limit of pressures, where $e^{-(P-c)/d} \ll 1$, *Eq. 1* converges to *Eq. 3* with $A =$

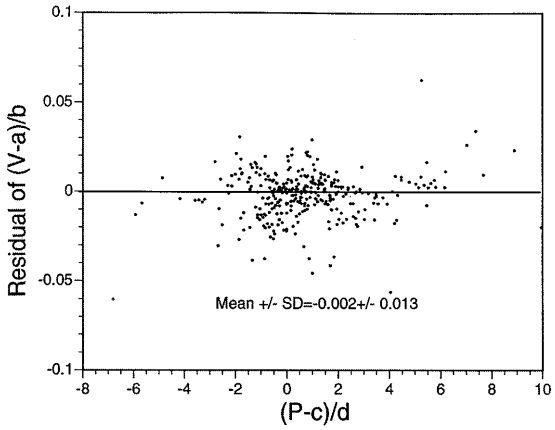

Fig. 5. Plot of residuals between measured data in Fig. 4 and *Eq. 1*.

$a + b$, $B = be^{c/d}$, and $k = d$. However, data including the low range of lung volumes is poorly fitted by *Eq. 3* (22), particularly for lungs with alveolar derecruitment and/or airway closure, such as in ARDS or pneumoconstriction (Figs. 1–3). To overcome this poor fitting at low lung volumes, investigators have combined *Eq. 3* with first- (3) or third-degree polynomials (16), resulting in improved curve fits, but at the expense of increased number of parameters with little or no physiological meaning.

A sigmoidal model of the static P-V curve of the form

$$V = \frac{TLC}{1 + k_1 e^{-k_2 P}} \quad (4)$$

where TLC, k_1, and k_2 are fitting parameters, was proposed by Paiva and co-workers (21) and was shown to be substantially better than *Eq. 3* in fitting P-V data for normal human lungs. *Equation 4*, however, forces the lower asymptote of this sigmoid to occur at zero volume, a requirement that limits its general applicability in diseased lungs, where the lower asymptote of lung volume may not be zero. The sigmoidal equation proposed here is equivalent to *Eq. 4* but includes a lower asymptote volume, a, with the constant k_1 being equivalent to $e^{c/d}$ and k_2 to $1/d$.

A hyperbolic-sigmoidal equation of the form

$$P = \frac{k_1}{V_M - V} + \frac{k_2}{V_m - V} + k_3$$

with five fitting parameters, k_1, k_2, k_3, V_M, and V_m (20), was also shown to fit extremely well ($R^2 > 0.997$) deflation P-V data from normal human lungs that extend to volumes below FRC. Those R^2 values, however, are not directly comparable to those reported in this communication, because they were obtained by curve fitting eye-smoothed lines traced over the data and not the measured data. Obviously, the higher number of parameters in the hyperbolic-sigmoidal equation (5 vs. 4 in *Eq. 1*) can be expected to yield better fitting to data.

It is noteworthy that the single equation proposed here (*Eq. 1*) could fit this diverse collection of P-V curves, particularly since *Eq. 1* is symmetrical[2] with respect to its inflection point. One would not expect a priori actual P-V data to have comparable symmetry, because the mechanical phenomena occurring at each end of the curve are very different. For example, during inflation the lower part of the curve probably reflects a combination of progressive recruitment of closed alveoli and elastic inflation of open lung regions. In contrast, the upper portion of the curve may correspond to approaching the maximal elastic distension of the fully recruited alveoli. Surface phenomena also have characteristics in inflation that are different from those in deflation. It is important to note that although *Eq. 1* may be symmetrical, the experimental data sets used were incomplete, in that they did not include data distributed throughout the entire range of the model. Most data sets are biased toward one asymptote. Deflation limbs typically include more data from the upper asymptote; inflation limbs tend to include more data from the lower asymptote. This limitation, however, does not seem to restrict the usefulness of *Eq. 1*, since in most cases it is not practical, or even desirable, to obtain complete data sets from both asymptotes. Deflation P-V curves generally stop at atmospheric pressure and, in the absence of lung disease and in the intact subject, may not approach the lower asymptote at this pressure. Similarly, it may not be possible to extend an inflation P-V curve to airway pressures high enough to reach the upper asymptote. Although all the data analyzed here fitted the model well, it is possible that *Eq. 1* might have to be modified to fit data sets that extend significantly onto both asymptotes.

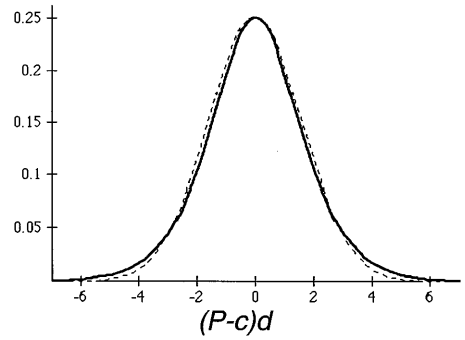

Fig. 6. Plots of a normal distribution (*Eq. 5*) with $\sigma \cong d\sqrt{\pi}$ (dashed line) and *Eq. 2*, derivative of *Eq. 1* (solid line).

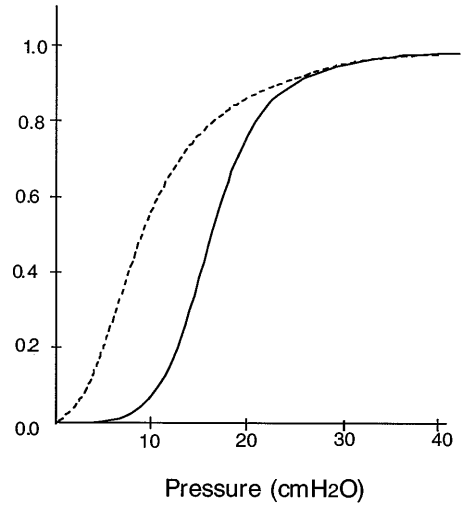

Fig. 7. Simulated inflation (solid line) and deflation (dashed line) P-V curves using mechanistic model in *Eq. 7*: $B = 1$, $k = 0.1$, and $d = 2.5$. To simulate difference in mean opening and closing pressures, parameter c was set to 15 cmH_2O for inflation and 5 cmH_2O for deflation.

[2] Strictly speaking, a function $F(x)$ is symmetrical with respect to the origin when $F(x) = -F(-x)$. In the case of *Eq. 1*, $F(x)$ with $x = (P - c)/d$ and transforming the function to $G(x) = F(x) - F(0)$, the function is symmetrical with respect to the inflection point ($P = c$ or $x = 0$), since $G(x) = -G(-x)$. This can be readily seen from the plot in Fig. 4 and by noting that the curvatures of the function at the lower and upper corner pressures are equal but have opposite signs.

One possible modification may come from the observation that the sigmoidal *Eq. 1* presented in dimensionless form as

$$\frac{V - a}{b} = \frac{1}{1 + e^{-(P-c)/d}} \quad (5)$$

has a derivative that is bell shaped and approximates to a normal distribution

$$\Pi = \frac{1}{\sigma[2\pi e^{-(P-c)/\sigma}]^2} \quad (6)$$

with standard deviation (σ) being approximately proportional to the parameter d

$$\sigma \cong d\sqrt{\pi}$$

Aside from their graphical similarity (Fig. 6), the derivatives of *Eqs. 5* and *6* have the following common characteristics: *1*) Both have a maximum value of 0.25 at $P = c$. *2*) Both are asymptotic to 0 as $(P - c)/d \rightarrow \pm\infty$. *3*) Both drop to 20% of the peak at $(P - c)/d \approx \pm 3$. *4*) Their integral from $-\infty$ to $+\infty$ are equal to unity. Thus *Eq. 1* in dimensionless form provides a closed-form approximation to the integral of normal distribution, an integral that has to be numerically calculated. This observation gives a basis to the intriguing possibility that the sigmoidal shape of the inflation limb of the P-V curve in ARDS could be reflecting the progressive recruitment of alveolar units with a distribution of Pao that follows a normal distribution. Similarly, the upper asymptote of the P-V curve could reflect the distribution of pressures at which all recruitable alveolar units become fully distended. If these distributions had similar characteristics, then the symmetry of *Eq. 1* could have a physiological basis.

Using these concepts, one can also formulate a P-V equation capable of fitting asymmetric data as the product of a normal-distribution-based recruitment function $R(P)$

$$R(P) = \frac{1}{1 + e^{-(P-c)/d}}$$

times a function representing the compliant properties of a recruited alveolus represented by an exponential function such as *Eq. 3*, yielding

$$V = \frac{TLC - Be^{-kP}}{1 - e^{-(P-c)/d}} \quad (7)$$

as illustrated in Fig. 7 for arbitrary parameters. As in the hyperbolic sigmoidal equation (22), the number of parameters has increased to five from four in *Eq. 1*. Although *Eq. 7* has the important advantage of having a mechanistic basis instead of being purely empirical, since *Eq. 1* can fit experimental data so well, the increasing number of parameters in *Eq. 7* may result in lower parameter sensitivity.

In summary, we have formulated a mathematical expression that fits with excellent accuracy ($R^2 = 0.997$) the inflation and deflation limbs of experimental and clinical P-V curves obtained under a variety of experimental and pathological conditions. The pressure and volume data are plotted normalized by parameters obtained from the model; the data tightly follow a single comprehensive relationship. This equation provides a method to systematically characterize P-V curves and objectively derive physiologically and clinically useful parameters such as vital capacity, maximal inspiratory volume, compliance at different inflation pressures, inflection pressure, and upper and lower corner pressures.

This work was supported by National Heart, Lung, and Blood Institute Grant HL-38267.

Present address of B. A. Simon: Dept. of Anesthesia and Critical Care Medicine, Johns Hopkins School of Medicine, Baltimore, MD 22222.

Address for reprint requests: J. G. Venegas, Dept. of Anesthesia (CLV-255), Massachusetts General Hospital, Boston, MA 02114.

Received 6 June 1997; accepted in final form 2 October 1997.

REFERENCES

1. **Adams, F. H., B. Towers, A. B. Osher, M. Ikegami, T. Fujiwara, and M. Nozaki.** Effects of tracheal instillation of natural surfactant in premature lambs. I. Clinical and autopsy findings. *Pediatr. Res*. 12: 841–848, 1978.
2. **Amato, M. B., C. S. Barbas, D. M. Medeiros, G. D. P. Schettino, F. G. Lorenzi, R. A. Kairalla, D. Deheinzelin, C. Morais, E. D. O. Fernandes, and T. Y. Takagaki.** Beneficial effects of the "open lung approach" with low distending pressures in acute respiratory distress syndrome. A prospective randomized study on mechanical ventilation. *Am. J. Respir. Crit. Care Med*. 152: 1835–1846, 1995.
3. **Bogaard, J. M., S. E. Overbeek, A. F. Verbraak, C. Vons, H. T. Folgering, D. M. T. Van, C. M. Roos, and P. J. Sterk.** Pressure-volume analysis of the lung with an exponential and linear-exponential model in asthma and COPD. Dutch CNSLD Study Group. *Eur. Respir. J*. 8: 1525–1531, 1995.
4. **Brody, J. S., S. Lahiri, M. Simpser, E. K. Motoyama, and T. Velasquez.** Lung elasticity and airway dynamics in Peruvian natives to high altitude. *J. Appl. Physiol*. 42: 245–251, 1977.
5. **Colebatch, H. J., I. A. Greaves, and C. K. Ng.** Pulmonary distensibility and ventilatory function in smokers. *Bull. Eur. Physiopath. Respir*. 21: 439–447, 1985.
6. **Colebatch, H. J., and C. K. Ng.** A longitudinal study of pulmonary distensibility in healthy adults. *Respir. Physiol*. 65: 1–11, 1986.
7. **Colebatch, H. J., and C. K. Ng.** Decreased pulmonary distensibility and pulmonary barotrauma in divers. *Respir. Physiol*. 86: 293–303, 1991.
8. **Colebatch, H. J., C. K. Ng, and N. Nikov.** Use of an exponential function for elastic recoil. *J. Appl. Physiol*. 46: 387–393, 1979.
9. **Colebatch, H. J. H., I. A. Creaves, and C. K. Ng.** Exponential analysis of elastic recoil and aging in healthy males and females. *J. Appl. Physiol*. 47: 693–691, 1979.
10. **Dreyfuss, D.** High inflation pressure pulmonary edema. Respective effects of high airway pressure, high tidal volume, and positive end-expiratory pressure. *Am. Rev. Respir. Dis*. 137: 1159–1164, 1988.
11. **Eidelman, D. H., H. Ghezzo, and J. H. Bates.** Exponential fitting of pressure-volume curves: confidence limits and sensitivity to noise. *J. Appl. Physiol*. 69: 1538–1541, 1990.
12. **Gattinoni, L., L. D'Andrea, P. Pelosi, G. Vitale, A. Pesenti, and R. Fumagalli.** Regional effects and mechanism of positive end-expiratory pressure in early adult respiratory distress syndrome. *JAMA* 269: 2122–2127, 1993.
13. **Gibson, G. J., J. B. Pride, J. Davis, and R. C. Schroter.** Exponential description of the static pressure-volume curve of normal and diseased lungs. *Am. Rev. Respir. Dis*. 120: 799–811, 1979.
14. **Greaves, I. A., and H. J. Colebatch.** Elastic behavior and structure of normal and emphysematous lungs post mortem. *Am. Rev. Respir. Dis*. 121: 127–136, 1980.

15. **Greaves, I. A., and H. J. Colebatch.** Large lungs after childhood asthma: a consequence of enlarged airspaces. *Aust. NZ J. Med*. 15: 427–434, 1985.
16. **Gugger, M., P. K. Wraith, and M. F. Sudlow.** A new method of analysing pulmonary quasi-static pressure-volume curves in normal subjects and in patients with chronic airflow obstruction. *Clin. Sci. (Lond.)* 78: 365–369, 1990.
17. **Ikegami, M., T. Hesterberg, M. Nozaki, and F. H. Adams.** Restoration of lung pressure-volume characteristics with surfactant: comparison of nebulization versus instillation and natural versus synthetic surfactant. *Pediatr. Res*. 11: 178–182, 1977.
18. **Kolobow, T.** Severe impairment in lung function induced by high peak airway pressure during mechanical ventilation: an experimental study. *Am. Rev. Respir. Dis*. 135: 312–315, 1987.
19. **Margulies, S. S., R. W. Schriner, M. A. Schroeder, and R. D. Hubmayr.** Static lung-lung interactions in unilateral emphysema. *J. Appl. Physiol*. 73: 545–551, 1992.
20. **Murphy, B. G., and L. A. Engel.** Models of the pressure-volume relationship of the human lung. *Respir. Physiol*. 32: 183–194, 1978.
21. **Paiva, M., J. C. Yernault, P. vanEerdeweghe, and M. Englert.** A sigmoidal model of the static volume-pressure curve of human lung. *Respir. Physiol*. 23: 317–323, 1975.
22. **Pengelly, L. D.** Curve-fitting analysis of pressure-volume characteristics of the lungs. *J. Appl. Physiol*. 42: 111–116, 1977.
23. **Petty, T. L., G. W. Silvers, G. W. Paul, and R. E. Stanford.** Abnormalities in lung elastic properties and surfactant function in adult respiratory distress syndrome. *Chest* 75: 571–574, 1979.
24. **Ranieri, V. M., L. Mascia, T. Fiore, F. Bruno, A. Brienza, and R. Giuliani.** Cardiorespiratory effects of positive end-expiratory pressure during progressive tidal volume reduction (permissive hypercapnia) in patients with acute respiratory distress syndrome. *Anesthesiology* 83: 710–720, 1995.
25. **Romero-Colomer, P., F. Manresa, and J. Escarrabill.** Pulmonary mechanics in methacholine induced asthma. *Allergol. Immunopathol. (Madr.)* 13: 135–141, 1985.
26. **Roupie, E., M. Dambrosio, G. Servillo, H. Mentec, S. el Atrous, L. Beydon, C. Brun-Buisson, F. Lemaire, and L. Brochard.** Titration of tidal volume and induced hypercapnia in acute respiratory distress syndrome. *Am. J. Respir. Crit. Care Med*. 152: 121–128, 1995.
27. **Saetta, M., and J. P. Mortola.** Exponential analysis of the lung pressure-volume curve in newborn mammals. *Pediatr. Pulmonol*. 1: 193–197, 1985.
28. **Salazar, E., and J. H. Knowles.** An analysis of pressure-volume characteristics of the lungs. *J. Appl. Physiol*. 19: 97–104, 1964.
29. **Schroter, R. C.** Quantitative comparisons of mammalian lung pressure-volume curves. *Respir. Physiol*. 42: 101–107, 1980.
30. **Simon, B. A., K. Tsuzaki, and J. G. Venegas.** Changes in regional lung mechanics and ventilation distribution after unilateral pulmonary artery occlusion. *J. Appl. Physiol*. 82: 882–891, 1996.
31. **Tsuno, K.** Histopathologic pulmonary changes from mechanical ventilation at moderately high airway pressures. *J. Appl. Physiol*. 69: 956–961, 1990.
32. **Venegas, J. G., and J. J. Fredberg.** Understanding the pressure cost of ventilation: why does high-frequency ventilation work? *Crit. Care Med*. 22: S48–S57, 1994.